Magnetic deflagration in Gd_5Ge_4

S. Velez,[1] J. M. Hernandez,[1] A. Fernandez,[1] F. Macià,[1] C. Magen,[2] P. A. Algarabel,[3] J. Tejada,[1] and E. M. Chudnovsky[1,4]
[1]*Facultat de Física, Universitat de Barcelona, Diagonal 645, 08028 Barcelona, Spain*
[2]*Instituto de Nanociencia de Aragón-ARAID, Universidad de Zaragoza, 50009 Zaragoza, Spain*
[3]*Instituto de Ciencia de Materiales de Aragón and Departamento de Física de la Materia Condensada, Universidad de Zaragoza and Consejo Superior de Investigaciones Científicas, 50009 Zaragoza, Spain*
[4]*Physics Department, Lehman College, The City University of New York, 250 Bedford Park Boulevard West, Bronx, New York 10468-1589, USA*
(Received 28 September 2009; revised manuscript received 19 December 2009; published 26 February 2010)

We report experiments on magnetic avalanches in the intermetallic compound Gd_5Ge_4. Kinetics of the avalanches have been studied and compared with the theory of magnetic deflagration. We show that the data fit well into the theoretical framework of deflagration. This adds Gd_5Ge_4 to the growing family of materials (that now includes molecular magnets and manganites) which exhibit this phenomenon. The "burning" of the metastable magnetic phase involves a magnetostructural transition alongside the reordering of spins.

DOI: 10.1103/PhysRevB.81.064437 PACS number(s): 75.60.Jk, 75.30.Kz, 82.33.Vx

I. INTRODUCTION

The unusual magnetic, magnetoelastic, and magnetocaloric properties of the intermetallic compound Gd_5Ge_4 have been intensively studied during the last decade.[1–9] This compound is paramagnetic above 128 K. Cooled down below 128 K it undergoes a transition into an antiferromagnetic (AFM) phase. Below 1 T field it remains antiferromagnetic down to zero temperature. The material has a layered crystal structure. It is believed that Gd spins inside each layer are aligned ferromagnetically while the layers order antiferromagnetically. When the field in access of 1 T is applied, the material becomes ferromagnetic (FM). The AFM-FM transition has been attributed to the first-order magneto-structural martensitic-like transformation in which the adjacent crystal nanolayers undergo shear displacements with respect to each other, resulting in the change in the exchange interaction between the layers from AFM to FM.[10] More recently, experiments were performed[11–13] that indicated that the low-temperature ground state of Gd_5Ge_4 may, in fact, be the FM one even at zero field. It has been argued that the onset of the zero-field FM ground state at low temperature is masked by the arrest of the crystal kinetics below 20 K. As a result, the low-temperature phase of Gd_5Ge_4 is a mixture of FM and AFM clusters with glassy properties.

Early magnetization measurements of Gd_5Ge_4 uncovered two modes of the AFM-FM transition on the application of the magnetic field.[2] The transition is rather gradual; that is, it takes place over an extended field range when a significant fraction of the FM phase is already present in the sample, or the temperature is relatively high, or the field is increasing slowly. The dynamics of such a gradual transition has been attributed to the nucleation and grows of FM clusters in the AFM environment that provides a variety of energy barriers and distribution of the nucleation rates.[14] On the contrary, if the sample is mostly made of the AFM phase, the low-temperature AFM-FM transition in the rapidly increasing magnetic field happens abruptly, within a very narrow field range. This avalanche-like process, that occurs when the field reaches a certain value, has striking similarity with avalanches observed in the magnetization curves of molecular magnets[15–18] and of some manganites.[19–21] The latter avalanches have been investigated and successfully described[22–29] within theory of magnetic deflagration.[30]

Deflagration is a physical term for slow burning that occurs, e.g., in a combustion engine when a chemical reaction in the fuel-air mixture is ignited by a spark of fire.[31] It is characterized by the propagation of a flame that separates the unburned substance ahead of the flame from the burned substance behind the flame. The flame moves at a constant speed well below the speed of sound as contrasted by the supersonic shock wave in the explosive burning. The kinetics of the deflagration is purely thermal. The heat released locally by the chemical reaction ignites the reaction in the nearby regions. This ensures the stability of the flame against fragmentation. The distance by which the heat diffuses during the time of the chemical reaction determines the width of the flame. The latter should be small compared to the dimensions of the sample; otherwise the heat may be escaping through the walls of the sample faster than it moves inside the material and the flame becomes extinguished. Experiments on chemical deflagration are irreversible as the substance becomes burned out. Also the parameters of the chemical deflagration, such as flammability and the reaction time, are usually fixed. On the contrary, magnetic deflagration is reversible (that is, the same sample can be reused many times), and it allows one to control the parameters of the process in a continuous manner. Besides being of interest on its own, it provides a powerful method of the study of the complex phenomenon of deflagration.

In magnetic deflagration, first observed in crystals of molecular magnets[22,23] and then in manganites,[25] the role of the chemical energy is played by the magnetic energy of the crystal. In molecular magnets, it is the Zeeman energy, while in manganites the free energy available for burning is a combination of the Zeeman energy and the energy of the metastable ordered magnetic phase. Note that not every first-order phase transformation would occur via deflagration. For instance, the avalanche-like growth of ice crystals in a supercooled water is driven by a different nucleation kinetics. Unlike deflagration it is not purely thermal. The same is true for

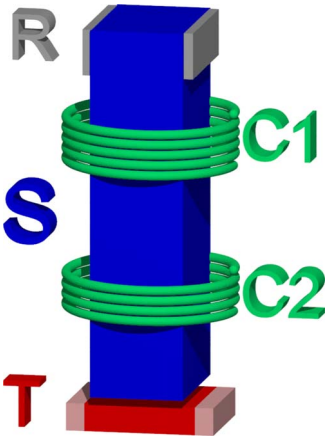

FIG. 1. (Color online) Experimental setup. The sample (s) is mounted on a sample holder with two pickup coils (C1 and C2) and one thermometer (t). Two electrical contacts at the upper edge of the sample are used to supply Joule heat and to measure the resistance. The assembly is introduced into the sample space of a commercial SQUID magnetometer.

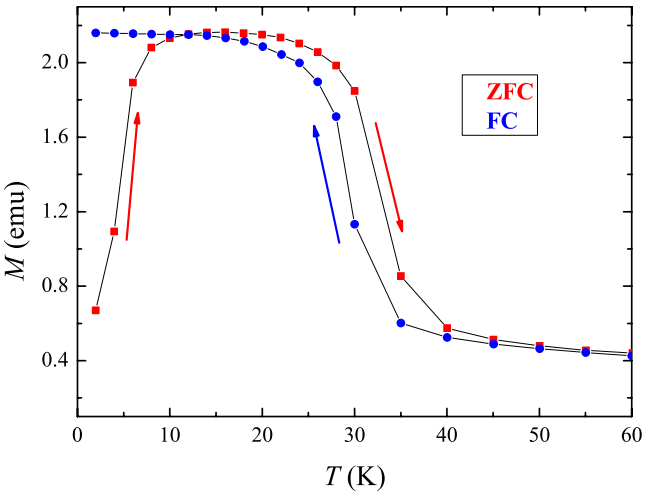

FIG. 2. (Color online) FC and ZFC magnetization of the Gd_5Ge_4 sample versus temperature. The mesalike ZFC curve is indicative of the AFM-FM transition on heating the sample in a 2 T field.

the nondissipative propagation of domain walls responsible for the magnetization reversal in pure FM materials. In a paramagnetic molecular magnet, the nondissipative slow collective nucleation of the magnetization reversal may occur due to weak dipolar interactions.[32] Faster magnetic relaxation may only occur via deflagration.[30] Similarly, in glassy magnetic materials, such as manganites and Gd_5Ge_4, fast nondissipative nucleation kinetics of a stable phase out of the metastable phase would be arrested by randomness. When the degree of metastability is not very high, this process in Gd_5Ge_4 occurs via random proliferation of FM clusters.[14] If, however, the application of the magnetic field results in a high degree of metastability, the magnetic transformation is likely to occur via deflagration.

The purpose of this work has been to investigate whether magnetic deflagration is responsible for the avalanches observed in the magnetization curve of Gd_5Ge_4. The structure of the paper is as follows. The experimental setup is described in Sec. II. Experimental data on the dynamics of the AFM-FM transition in Gd_5Ge_4 are presented in Sec. III. Comparison with the theory of deflagration is done in Sec. IV. We show that the data fit well into the theoretical framework of deflagration. This adds Gd_5Ge_4 to the growing family of materials that exhibit magnetic deflagration. The "burning" of the metastable phase is likely to involve not just the reordering of spins but also a structural transition.

II. EXPERIMENTAL SETUP

The alloy with nominal composition Gd_5Ge_4 was synthesized by arc melting of 99.9 wt % pure Gd and 99.9999 wt % pure Ge in a high-purity argon atmosphere. The details on the sample preparation and characterization can be found in Ref. 33. A polycrystalline sample of Gd_5Ge_4, with dimensions approximately $4\times1\times1$ mm^3 was placed inside a plastic tube (see Fig. 1). Two pick-up coils (C1 and C2) of five turns each were wound around the tube near the two edges of the sample. The voltage drop in each coil is proportional to the time derivative of the magnetization change of the part of the sample near each coil. At one edge of the sample we placed a calibrated Cernox thermometer (T) in order to monitor the temperature changes in the sample. Resolution time of the thermometer was about 10 ms. Two electrical contacts at the opposite edge of the sample allowed us to measure the resistivity of the sample and also to heat the sample by a dc-current pulse. The assembly was placed within the bore of a commercial superconducting magnet system capable of producing magnetic fields up to 5 T and temperatures in the range from 300 down to 1.8 K. The magnetic field was applied along the longest dimension of the sample. The data-acquisition card ([recording coil voltages, thermometer resistance, sample resistance, superconducting quantum interference device (SQUID) signal, and applied magnetic field] was triggered together with an avalanche produced by a weak heat pulse.

In all our measurements of the field dependence and temperature dependence of the magnetization we were using SQUID as a magnetometer. For these conventional measurements the time resolution is in the ballpark of tens of seconds due to the time needed to move the sample across the three pick-up coils. For the measurements of the avalanches, however, we used a completely different method. Since avalanches were generated at a constant field, measurement of the magnetization did not require any motion of the sample. The magnetization was monitored continuously by directly reading the voltage from the SQUID voltmeter. The resolution time in this case is better than a millisecond.

III. RESULTS

Temperature dependence of the magnetization for the field-cooled (FC) and zero-field-cooled (ZFC) samples of Gd_5Ge_4 in the low-temperature range is shown in Fig. 2. Below 128 K the material is antiferromagnetic. When the

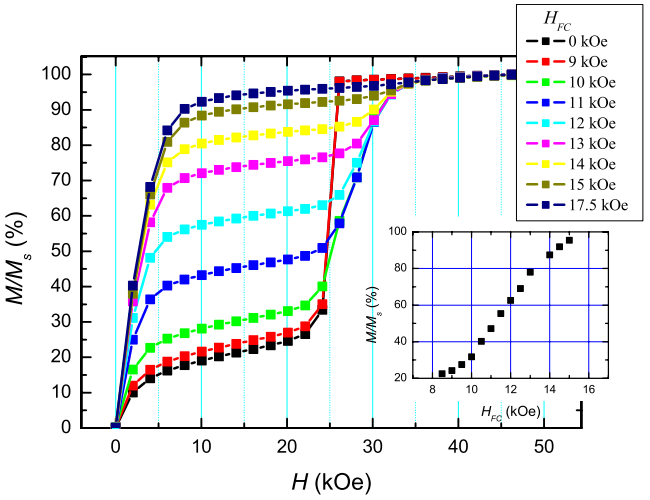

FIG. 3. (Color online) Isothermal (T=2 K) magnetization curves of the Gd_5Ge_4 sample cooled in the presence of the magnetic field, H_{FC}. At low H_{FC}, when the initial state is mostly antiferromagnetic, the magnetization changes in an avalanche-like process. Avalanches occur only at low temperatures and high-field-sweep rates. The inset shows the initial magnetization vs field, achieved in a FC process at a cooling rate of 10 K/min.

sample is further cooled down in a field larger than 1 T, it exhibits a gradual transition into an FM phase within the temperature range from 40 to 20 K, as is seen in the FC curve. When the same sample is cooled down in a weak magnetic field, it has a very small magnetization at 2 K, apparently due to the arrest of the kinetics that freezes the metastable AFM phase instead of taking the entire sample to the FM ground state. This state has been referred to as a mixture of AFM clusters and randomly oriented FM clusters with glassy behavior.[11,12] Heating the sample in a 2 T field unfreezes the arrested kinetics, leading to the gradual onset of ferromagnetism in the entire sample above 8 K, as is seen in the ZFC curve. On further temperature increase the sample re-enters the AFM phase between 20 and 40 K. The characteristic mesa in $M(T)$ between 10 and 20 K is indicative of the AFM-FM transition. These data are in accordance with the data on Gd_5Ge_4 cited in the Introduction.

Also in accordance with the previously cited data are our measurements of the magnetization curve. As the transformation from the initial mixed state into the FM state is driven by relaxation to the minimum of the free energy, the magnetization curves depend on both the temperature and the field-sweep rate.[3] Magnetization curves that exhibit avalanches are totally reproducible. We studied the dependence of the AFM-FM transition on the initial frozen state at low temperature. The initial state depends drastically on the field, H_{FC}, that had been applied when the sample was cooled down. This field determines how much of the FM phase is initially present in the system. Ultimately it determines whether the transition into the FM state is smooth or it occurs via an avalanche. The cooling rate is another important parameter. In our experiment it was kept constant at 10 K/min. The field was swept at 300 Oe/s. Figure 3 shows isothermal magnetization curves obtained after cooling the sample down to 2 K in different magnetic fields H_{FC} ranging from H_{FC}=0 kOe to H_{FC}=22 kOe. Different curves correspond to different initial states. For H_{FC} above 14 kOe, the magnetization curves are typical of randomly oriented FM clusters. Lower cooling fields allow the sample to remain partially in the AFM state with a significant amount of AFM clusters that reveal themselves as a knee in the magnetization curve above 25 kOe. This knee apparently corresponds to the gradual transformation of the AFM phase into the FM phase upon increasing the field. For H_{FC} below 10 kOe the amount of metastable AFM phase is close to the value obtained through zero-field cooling. Such an initial state is sufficient to ignite an avalanche-like transformation of the whole sample into the FM phase. The initial value of the AFM phase can be estimated at each temperature and magnetic field from the ratio of M and its value (at the same temperature and field) for the sample prepared in the FM state. The inset of Fig. 3 shows the initial magnetization as a function of the field in the FC process.

Figures 2 and 3 are given to demonstrate that our Gd_5Ge_4 sample exhibits same properties that have been reported in literature and furthermore to show our ability to control the initial state at low temperature. In the next set of measurements presented we focus our attention on avalanches. In our experiments we produced magnetic avalanches by two methods. In the first method avalanches appear spontaneously by sweeping the magnetic field (as seen in Fig. 3). Initial rough measurements suggested that the nucleation occurred close to the middle of the sample; the signals of the two coils were almost simultaneous. The detected small time difference indicated that some propagation of the signal was involved. To avoid large error, the speed of the avalanche in this case was deduced from the time width of the signal. The result was very similar to that deduced from the time difference in the two coils when the avalanches were ignited at one of the edges of the sample. Further proof of the propagation was obtained by playing with the positions of the coils. The thermometer detected temperatures of the order of 6–7 K for avalanches ignited at 2 K. The field at which the avalanche spontaneously takes place, H_{ava}, in a field-sweep experiment has strong dependence on the initial temperature of the sample, varying from 23 kOe at 2 K to 17 kOe at 6 K. This dependence is shown in Fig. 4.

Several experiments with different locations of the coils indicated that avalanches moved through the sample. To develop a better accuracy in determining the speed of the moving front, we implemented a method in which avalanches were definitively ignited at one edge of the sample. A thermal pulse was delivered to that edge at the ignition field, H_{ign}, that was kept constant. Figure 5 illustrates the measuring capabilities of the setup. At a constant magnetic field the variation of the total magnetization can be monitorized by continuously reading the voltage at the SQUID voltmeter. Time evolution of the SQUID magnetization (black straight line) together with the sample temperature (red dashed line) are plotted. A striking feature of the plot is the linear dependence of the SQUID magnetization on time. Note that a linear time dependence of the total magnetization does not correspond to any known relaxation phenomenon. This feature is, therefore, indicative of the avalanche moving through the sample at a constant speed. Additionally, the signal of the

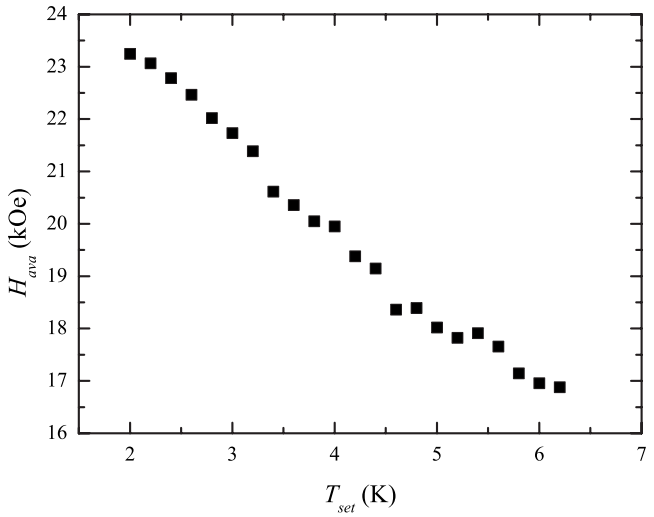

FIG. 4. Temperature dependence of the field at which the avalanche spontaneously occurs. The Gd_5Ge_4 sample was cooled in a zero magnetic field down to $T=2$ K.

two pick-up coils was monitored. The inset in Fig. 5 shows the time evolution of the magnetization measured by the two coils. The delay from one coil to the other shows that the avalanche propagates through the sample. The rise of the sample temperature correlates with the magnetization signal (the time response of the thermometer is of the order of 10 ms). The maximum measured temperature, however, is not expected to correspond to the actual sample temperature because of the narrow width and rapid motion of the deflagration front and also due to imperfect coupling between the sample and the thermometer.

The speed of the avalanche can be computed from independent measurements: From the duration of the coil signal,

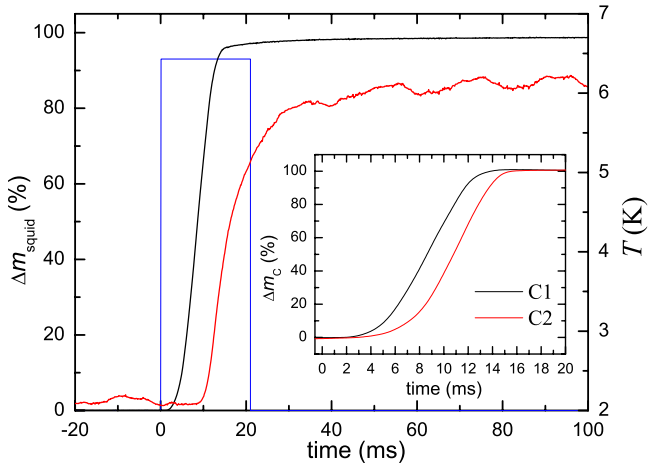

FIG. 5. (Color online) Time evolution of the variation of the magnetization of the sample detected by the SQUID voltmeter (black straight line) and sample temperature (red dashed line) during an avalanche at the initial temperature $T=2$ K and $H_{ign}=20$ kOe. The blue curve indicates the duration of the heat pulse. The Gd_5Ge_4 sample was cooled down in a zero magnetic field. The inset shows signals in the two pick-up coils C1 (black) and C2 (red).

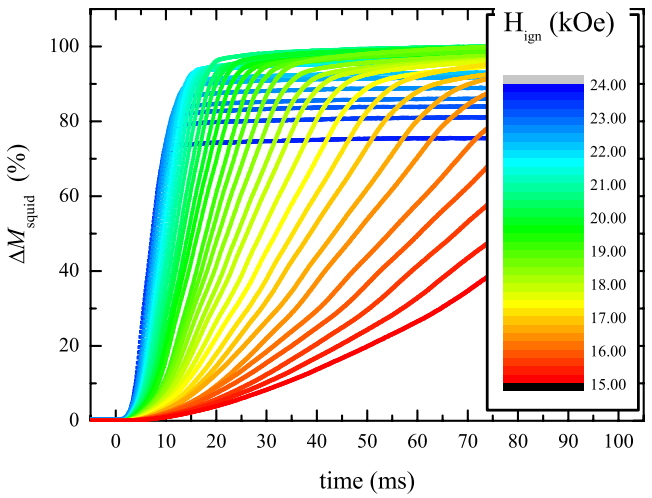

FIG. 6. (Color online) Time evolution of the variation of the magnetization of the Gd_5Ge_4 sample detected by the SQUID voltmeter after application of various ignition fields. The sample was cooled down to $T=2$ K in a zero magnetic field.

from the time difference between the maxima in the two coils, and from the SQUID signal. These definitions turned out to be equivalent. Figure 6 shows the time evolution of the SQUID magnetization at different ignition fields. The larger the ignition field, the faster is the avalanche. All curves were measured with the same SQUID scale to simplify comparison. In nearly all curves the magnetization varied from zero to saturation, meaning that the initial and final states were the same. Magnetization measurements before and after the avalanche showed that avalanches resulted in the full magnetization (i.e., the final state was totally FM). However, avalanches at higher fields $H_{ign}>21$ kOe had slightly different initial state as the sample had partially relaxed before the avalanche. Therefore the measured variation of the magnetization dropped to 75%.

The ignition field dependence of the avalanche speed, derived from the curves of Fig. 6, is plotted in Fig. 7. A sort of saturation at higher fields has been observed that corresponds to avalanches beginning from a slightly relaxed initial state as described above. The heat released during the abrupt crystallographic transition corresponds to the difference between the free energy of the metastable AFM state and stable FM state, plus the Zeeman energy $E=g\mu_B H$ per spin of the ferromagnetic cluster. The inset in Fig. 7 shows the ignition field dependence of the maximum registered temperature. As expected, the temperature goes up with the increasing ignition field, that is, fast avalanches generate more heat. Same as for the speed, the maximum temperature exhibits saturation at high ignition fields. The experiment was repeated by cooling the sample in the presence of the 10 kOe field (red circles in Fig. 7). The ZFC and FC results are similar. The only (anticipated) difference is the shift to lower velocities and consequently to the lower heat released by the avalanche. To better illustrate the FC effect we plotted together in Fig. 8 the speed of the avalanche and the initial magnetization before the heat pulse was applied. (The difference from the inset in Fig. 3 is due to the 22 kOe field applied each time before the avalanche was ignited.) There is a clear

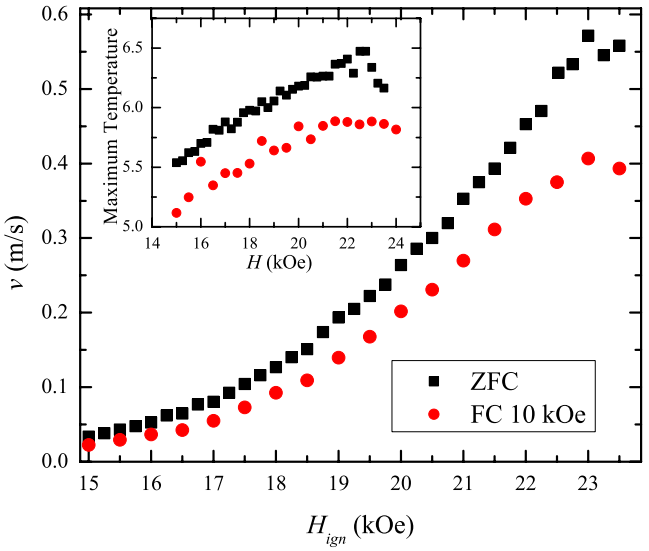

FIG. 7. (Color online) Ignition field dependence of the avalanche speed in the Gd_5Ge_4 sample, obtained from Fig. 6. Avalanches were ignited at $T=2$ K. The inset shows the maximum measured temperature for each avalanche.

correlation between the two: The initial relaxation reduces "flammability" of the crystal. These results are similar to the results on molecular magnets[24,27] and on manganites.[25]

In order to distinguish between the temperature rise due to the heat pulse itself and the temperature rise due to the avalanche we plotted Fig. 9 the temperature measured by the thermometer for two different situations: During the avalanche that transformed the sample from a metastable AFM-FM mixture into a stable FM phase (black squares) and when the same heat pulse was delivered to the FM sample long after the avalanche had occurred (red circles). The figure shows that the heat pulse itself barely heats the sample by 1–1.5 K, whereas the temperature rise due to the avalanche does not depend on the initial sample temperature and reaches a value of 6 K for $H_{ign}=19$ kOe.

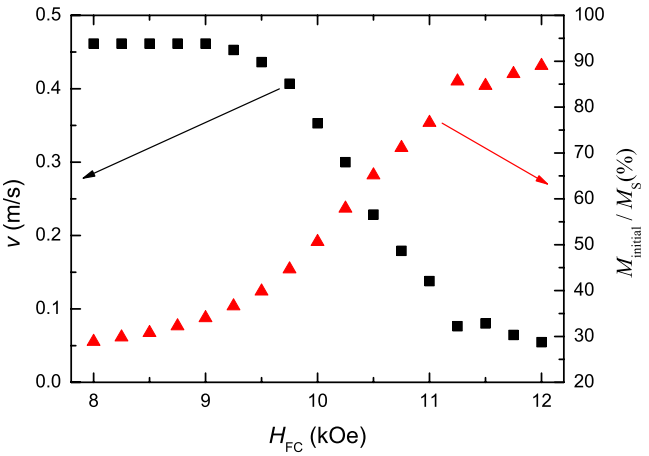

FIG. 8. (Color online) Dependence of the avalanche velocity (black squares) on the field used in the FC process and the initial magnetization (red triangles). Avalanches in a Gd_5Ge_4 sample were ignited at 2 K and 22 kOe field.

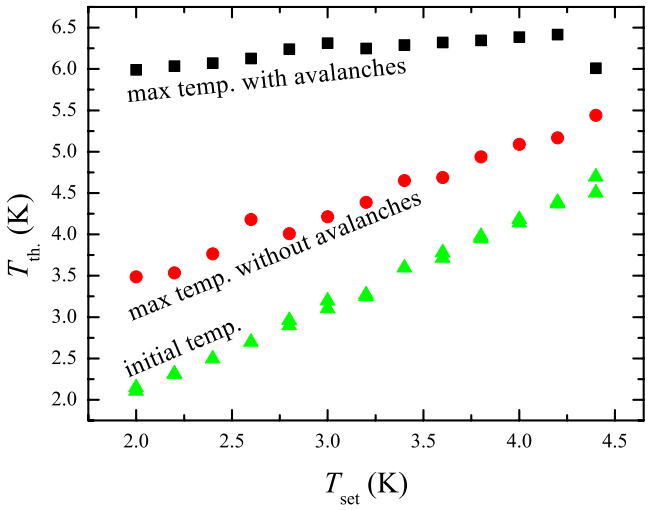

FIG. 9. (Color online) Maximum temperature variation during the avalanche triggered by a heat pulse (black squares) and due to the heat pulse itself when it is delivered to the FM sample (red circles). The Gd_5Ge_4 sample was ZFC down to $T=2$ K. The experiment was conducted at $H=19$ kOe.

IV. DISCUSSION

We now compare properties of the observed avalanches with the theory of magnetic deflagration. One important parameter is the temperature of the flame, T_f. It can be computed from the equation

$$\Delta E = \int_{T_i}^{T_f} C(T)dT, \tag{1}$$

where ΔE is the released metastable energy, T_i is the initial temperature of the sample, and $C(T)$ is the specific heat. In the temperature range of interest, $C(T)=\alpha T^3$ (with α being a constant[1]). This points toward phonon-dominated processes, same as in molecular magnets. In this case, the theoretical formula[30]

$$T_f = \frac{\Theta_D}{\pi}\left(\frac{5n_m\Delta E}{3k_B\Theta_D}\right)^{1/4}, \tag{2}$$

has been proven to provide a good estimate of T_f. Here Θ_D is the Debye temperature of the material and n_m is the fraction of the metastable phase. The Debye temperature of Gd_5Ge_4 is[1] 120 K (as compared to only 30 K in the Mn-12 molecular magnet). Assuming that the parameter ΔE has the same order of magnitude as the energy barrier, which can be estimated at 200 K from the FC-ZFC curves, one obtains from Eq. (2) T_f in the ballpark of 30 K (as compared to the typical value of 10 K in molecular magnets). This high value of T_f should not be surprising given the strong magnetocaloric effect in Gd_5Ge_4.

The first test of the magnetic deflagration is the width of the flame, which must be small compared to the dimensions of the sample. It is related to the thermal diffusivity κ and the velocity of the flame v by the formula $\delta \sim \kappa(T_f)/v$. Taking $\kappa(30\ K) \sim 10^{-5}$ m^2/s from Ref. 34 we obtain in our range of velocities, 0.1–1 m/s, the value of δ between 0.01 and 0.1

mm, which is small compared to the diameter of the sample, $d \sim 1$ mm. Such a flame can, indeed, be formed inside the sample and can move through the sample.

The next test is the condition of the instability of the metastable state against deflagration. It reads as[30]

$$\Gamma(T) > \frac{8k(T)k_B T^2}{U\Delta E n_m d^2}, \tag{3}$$

where $k(T)$ is thermal conductivity, U is the energy barrier, and $\Gamma(T)$ is the rate of the spontaneous decay of the metastable state. To apply this formula to Gd_5Ge_4, we write $n_m = n_{AFM}$, $n_{AFM}+n_{FM}=1$,

$$\Gamma n_{AFM} = -\frac{dn_{AFM}}{dt} = \frac{dn_{FM}}{dt} = \frac{dn_{FM}}{dH}\frac{dH}{dt}. \tag{4}$$

Condition (3) must be fulfilled when the temperature of the spontaneously "burning" sample unblocks the arrest of the kinetics responsible for the AFM-FM transformation, $U/(k_B T) \sim 25$. According to the FC-ZFC measurements it occurs at $T_B \sim 7$ K. Writing $k(T) \equiv \kappa(T)C(T) = \kappa(T)\alpha T^3$, $\Delta E = \alpha T_f^4/4$, we obtain from Eq. (3)

$$\frac{dn_{FM}}{dH} > \frac{\kappa(T_B)}{d^2(dH/dt)}\left(\frac{T_B}{T_f}\right)^4, \tag{5}$$

where we omitted unessential factor close to one. Since dn_{FM}/dH is always limited to a maximum of about 0.1/kOe (see the magnetization curve in Fig. 3), this formula explains why avalanches can only be ignited at a high-field-sweep rate dH/dt and in samples of sufficient size. Substitution into Eq. (5) of $dn_{FM}/dH \sim 0.1/\text{kOe}$, $T_B \sim 7$ K, $T_f \sim 30$ K, $l \sim 1$ mm, and[34] $\kappa(7K) \sim 3 \times 10^{-5}$ m^2/s, gives the required dH/dt in the ballpark of 1 kOe/s, which is the right order of magnitude for the sweep-field rate that is capable of igniting the avalanche.

Note that dn_{FM}/dH curves are different for different initial temperatures of the sample. At a fixed field-sweep rate, condition (5) is achieved in a smaller field when the initial temperature of the sample is higher. This explains the dependence of the field of the avalanche on the initial temperature [Fig. 4]. Notice also that T_f goes down with the decreased amount of the AFM phase available for burning. This occurs at higher initial temperatures and/or higher H_{FC}, reducing the flammability of the material according to Eq. (5). It explains why avalanches are only observed at low initial temperature of the sample and in samples cooled down in low H_{FC} [see Fig. 3].

Finally, it is interesting to know whether the theory of deflagration can provide the correct ballpark for the velocity of the avalanche and the correct trend for the dependence of the velocity on the magnetic field at which the avalanche occurs [Fig. 7]. The expression for the velocity in the theory of deflagration is[30]

$$v \sim [(k_B T_f/U)\kappa(T_f)\Gamma(T_f)]^{1/2}, \tag{6}$$

where $\Gamma(T) = \nu \exp[-U/(k_B T)]$, and ν is the attempt frequency. Substituting here $T_f \sim 30$ K, $U \sim 200$ K, $\kappa(T_f) \sim 10^{-5}$ m^2/s, and the value of $\nu \sim 10^7$ s^{-1} that is typical for magnetic transitions, one gets $\Gamma \sim 10^4$ s^{-1} and $v \sim 0.1$ m/s, in accordance with our experimental finding. Fast increase of v in the magnetic field at which the avalanche occurs can then be naturally attributed to the decrease in the energy barrier U that results in the exponential increase of Γ. Thus, all data on magnetic avalanches in Gd_5Ge_4 fit well within the framework of magnetic deflagration.

V. CONCLUSION

We have presented experimental evidence that the field-induced AFM-FM magnetostructural transformation in Gd_5Ge_4 occurs via an avalanche that traverses the sample at a speed 0.1–1 m/s. This process is driven by the heat conductance and it closely resembles the magnetic deflagration observed in molecular magnets and manganites.[22–29] The dependence of avalanches on the initial state, initial temperature, and magnetic field agrees with the theory of deflagration.[30] Since magnetic transition in Gd_5Ge_4 also involves structural transformation, it represents an interesting example of the magnetostructural deflagration.

ACKNOWLEDGMENTS

The authors thank L. Morellon for his collaboration. S.V., F.M., and J.M.H. thank Spanish Ministry of Education and Science for the research grant. J.M.H. thanks University of Barcelona for the Ramon y Cajal research contract. J.T. thanks Catalan Institute of Research and Advanced Studies for the financial support. P.A. acknowledges financial support by the Aragon Regional Government (through Project No. E26). E.M.C. acknowledges support from the University of Barcelona and from the U.S. National Science Foundation through Grant No. DMR-0703639.

[1] E. M. Levin, V. K. Pecharsky, K. A. Gschneidner, Jr., and G. J. Miller, Phys. Rev. B **64**, 235103 (2001).

[2] E. M. Levin, K. A. Gschneidner, Jr., and V. K. Pecharsky, Phys. Rev. B **65**, 214427 (2002).

[3] V. Hardy, S. Majumdar, S. Crowe, M. R. Lees, D. McK. Paul, L. Herve, A. Maignan, S. Hebert, C. Martin, C. Yaicle, M. Hervieu, and B. Raveau, Phys. Rev. B **69**, 020407(R) (2004).

[4] H. Tang, V. K. Pecharsky, K. A. Gschneidner, Jr., and A. O. Pecharsky, Phys. Rev. B **69**, 064410 (2004).

[5] M. K. Chattopadhyay, M. A. Manekar, A. O. Pecharsky, V. K. Pecharsky, K. A. Gschneidner, Jr., J. Moore, G. K. Perkins, Y. V. Bugoslavsky, S. B. Roy, P. Chaddah, and L. F. Cohen, Phys. Rev. B **70**, 214421 (2004).

[6] Ya. Mudryk, A. P. Holm, K. A. Gschneidner, Jr., and V. K. Pecharsky, Phys. Rev. B **72**, 064442 (2005).
[7] Z. W. Ouyang, V. K. Pecharsky, K. A. Gschneidner, Jr., D. L. Schlagel, and T. A. Lograsso, Phys. Rev. B **76**, 134406 (2007).
[8] Z. W. Ouyang, H. Nojiri, S. Yoshii, G. H. Rao, Y. C. Wang, V. K. Pecharsky, and K. A. Gschneidner, Jr., Phys. Rev. B **77**, 184426 (2008).
[9] C. Magen, Z. Arnold, L. Morellon, Y. Skorokhod, P. A. Algarabel, M. R. Ibarra, and J. Kamarad, Phys. Rev. Lett. **91**, 207202 (2003).
[10] D. Paudyal, V. K. Pecharsky, K. A. Gschneidner, Jr., and B. N. Harmon, Phys. Rev. B **75**, 094427 (2007).
[11] S. B. Roy, M. K. Chattopadhyay, P. Chaddah, J. D. Moore, G. K. Perkins, L. F. Cohen, K. A. Gschneidner, Jr., and V. K. Pecharsky, Phys. Rev. B **74**, 012403 (2006).
[12] S. B. Roy, M. K. Chattopadhyay, A. Banerjee, P. Chaddah, J. D. Moore, G. K. Perkins, L. F. Cohen, K. A. Gschneidner, Jr., and V. K. Pecharsky, Phys. Rev. B **75**, 184410 (2007).
[13] L. S. Sharath Chandra, S. Pandya, P. N. Vishwakarma, D. Jain, and V. Ganesan, Phys. Rev. B **79**, 052402 (2009).
[14] G. K. Perkins, J. D. Moore, M. K. Chattopadhyay, S. B. Roy, P. Chaddah, V. K. Pecharsky, K. A. Gschneider, Jr., and L. F. Cohen, J. Phys.: Condens. Matter **19**, 176213 (2007).
[15] C. Paulsen and J.-G. Park, in *Quantum Tunneling of Magnetization—QTM'94*, edited by L. Gunther and B. Barbara (Kluwer, Dordrecht, Netherlands, 1995), pp. 189–207.
[16] F. Fominaya, J. Villain, P. Gandit, J. Chaussy, and A. Caneschi, Phys. Rev. Lett. **79**, 1126 (1997).
[17] E. del Barco, J. M. Hernandez, M. Sales, J. Tejada, H. Rakoto, J. M. Broto, and E. M. Chudnovsky, Phys. Rev. B **60**, 11898 (1999).
[18] M. Bal, J. R. Friedman, K. Mertes, W. Chen, E. M. Rumberger, D. N. Hendrickson, N. Avraham, Y. Myasoedov, H. Shtrikman, and E. Zeldov, Phys. Rev. B **70**, 140403 (2004).
[19] R. Mahendiran, A. Maignan, S. Hebert, C. Martin, M. Hervieu, B. Raveau, J. F. Mitchell, and P. Schiffer, Phys. Rev. Lett. **89**, 286602 (2002).
[20] L. Ghivelder, R. S. Freitas, M. G. das Virgens, H. Martinho, L. Granja, G. Leyva, P. Levy, and F. Parisi, Phys. Rev. B **69**, 214414 (2004).
[21] L. Ghivelder and F. Parisi, Phys. Rev. B **71**, 184425 (2005).
[22] Y. Suzuki, M. P. Sarachik, E. M. Chudnovsky, S. McHugh, R. Gonzalez-Rubio, N. Avraham, Y. Myasoedov, E. Zeldov, H. Shtrikman, N. E. Chakov, and G. Christou, Phys. Rev. Lett. **95**, 147201 (2005).
[23] A. Hernández-Mínguez, J. M. Hernandez, F. Macià, A. García-Santiago, J. Tejada, and P. V. Santos, Phys. Rev. Lett. **95**, 217205 (2005).
[24] S. McHugh, R. Jaafar, M. P. Sarachik, Y. Myasoedov, A. Finkler, H. Shtrikman, E. Zeldov, R. Bagai, and G. Christou, Phys. Rev. B **76**, 172410 (2007).
[25] F. Macià, A. Hernández-Mínguez, G. Abril, J. M. Hernandez, A. García-Santiago, J. Tejada, F. Parisi, and P. V. Santos, Phys. Rev. B **76**, 174424 (2007).
[26] F. Macià, J. M. Hernandez, J. Tejada, S. Datta, S. Hill, C. Lampropoulos, and G. Christou, Phys. Rev. B **79**, 092403 (2009).
[27] S. McHugh, B. Wen, X. Ma, M. P. Sarachik, Y. Myasoedov, E. Zeldov, R. Bagai, and G. Christou, Phys. Rev. B **79**, 174413 (2009).
[28] S. McHugh, R. Jaafar, M. P. Sarachik, Y. Myasoedov, A. Finkler, E. Zeldov, R. Bagai, and G. Christou, Phys. Rev. B **80**, 024403 (2009).
[29] F. Macià, G. Abril, J. M. Hernandez, and J. Tejada, J. Phys.: Condens. Matter **21**, 406005 (2009).
[30] D. A. Garanin and E. M. Chudnovsky, Phys. Rev. B **76**, 054410 (2007).
[31] See, e.g., I. Glassman, *Combustion* (Academic Press, New York, 1996).
[32] D. A. Garanin and E. M. Chudnovsky, Phys. Rev. Lett. **102**, 097206 (2009).
[33] C. Magen, L. Morellon, P. A. Algarabel, C. Marquina, and M. R. Ibarra, J. Phys.: Condens. Matter **15**, 2389 (2003).
[34] S. Fujieda, Y. Hasegawa, A. Fujita, and K. Fukamichi, J. Appl. Phys. **95**, 2429 (2004).